



# University of HUDDERSFIELD

## University of Huddersfield Repository

Sambo, Bello, Bevan, Adam and Pislaru, Crinela

A novel application of image processing for the detection of rail surface RCF damage and incorporation in a crack growth model

### Original Citation

Sambo, Bello, Bevan, Adam and Pislaru, Crinela (2016) A novel application of image processing for the detection of rail surface RCF damage and incorporation in a crack growth model. In: International Conference on Railway Engineering 2016 (ICRE), 12th - 13th May 2016, Brussels, Belgium.

This version is available at <http://eprints.hud.ac.uk/id/eprint/28497/>

The University Repository is a digital collection of the research output of the University, available on Open Access. Copyright and Moral Rights for the items on this site are retained by the individual author and/or other copyright owners. Users may access full items free of charge; copies of full text items generally can be reproduced, displayed or performed and given to third parties in any format or medium for personal research or study, educational or not-for-profit purposes without prior permission or charge, provided:

- The authors, title and full bibliographic details is credited in any copy;
- A hyperlink and/or URL is included for the original metadata page; and
- The content is not changed in any way.

For more information, including our policy and submission procedure, please contact the Repository Team at: [E.mailbox@hud.ac.uk](mailto:E.mailbox@hud.ac.uk).

<http://eprints.hud.ac.uk/>

# A novel application of image processing for the detection of rail surface RCF damage and incorporation in a crack growth model

B. Sambo, A. Bevan, C. Pislaru

Institute of Railway Research, University of Huddersfield, UK.

**Keywords:** surface crack detection; feature extraction; image processing segmentation; railway safety; rolling contact fatigue crack growth simulation.

## Abstract

The paper presents the development of an intelligent image processing algorithm capable of detecting fatigue defects from images of the rail surface. The links between the defect detection algorithm and 3D models for rail crack propagation are investigated, considering the influence of input parameters (materials, vehicle characteristics, loading conditions).

The dynamic behaviour at the wheel-rail interface resulting in contact forces responsible for stressing and straining the rail material are imported from vehicle dynamics simulations. The integration of the simulated results from vehicle dynamics, contact and fracture mechanics models offer more reliable estimation of the stress intensity factors (SIF). Also the sensitivity analysis related to materials, vehicle characteristics, and loading conditions will provide further understanding of the factors that influence crack propagation in rails such as shear stresses, hydraulic pressure, fluid entrapment and squeeze film effect.

This novel application of image processing for the detection of rail surface rolling contact fatigue (RCF) damage and automatic incorporation in a crack growth model represents an important contribution to the development of modern techniques for non-destructive rail inspection. This will result in improved planning/scheduling of future rail maintenance (e.g. rail grinding, renewal), less disruptions and reduced track maintenance costs in rail industry.

## 1. Introduction

A large proportion of derailments and service disruptions are caused by track-related issues. Increases in axle loads, vehicles primary yaw suspension stiffness, wheel-rail conicity and capacity have resulted in greater damage to the track. RCF cracks initiate in the surface or subsurface of rails and can propagate to cause rail failure, impacting on safety, maintenance and costs. The vision for Great Britain (GB) railway, as set out in the Rail Technical Strategy [1], emphasises the need for improvements in condition monitoring of rail assets from current inspection methods to more automated procedures (intelligent ‘self-monitoring’ systems) aimed at improving the efficiency of maintenance planning. To achieve this, manual inspection of rail defects should be replaced by more efficient non-destructive evaluation (NDE) techniques using visual cameras, ultrasonic probes, eddy currents etc. Papaelias et al [2] mentioned that

the high-speed inspection of rails can be achieved with automated vision techniques and hybrid systems based on the simultaneous use of pulsed eddy current probes and conventional ultrasonic probes. Eddy current methods employ techniques such as Field Gradient Imaging, Alternating Current Field Measurement (ACFM), and Electromagnetic Acoustic Transducers (EMATs). The detection of surface defects is sensitive to lift off variation, which is practically problematic to control [3]. Hashmi et al [4] detected rail head spalling by morphological operations and optimal adaptive thresholding methods but did not extract the geometrical features of the detected defects.

Wenyu et al [5] presented a shape based image processing algorithm which uses average smoothing filtering, thresholding and morphological opening for only detecting and classifying defects.

A more robust visual inspection system (VIS) was described by Quingyoung et al [6]. It was focused on the local contrast enhancement in addition to segmentation by thresholding algorithm. However feature extraction of detected defects was not investigated. In [7] a VIS based on contrast enhancement, noise filtration and defect localisation by analysing the projection profile of the mean intensity of each transversal and longitudinal line pair forming a suspect rectangle (SR) was described. Defects were segmented using a thresholding rule. The method is capable of only the extraction of longitudinal and transverse positions of detected defects.

Liu [8] used mean filtering, dynamic thresholding and morphological fill, followed by erosion for detection of defects. Furthermore a feature extraction was performed but limited to only the length of defects and calculations of percentage wear. Development of defect detection based on known properties of rail image was presented in [9]. However the authors only highlighted the application of filters for estimating the location and rectangular area of the defect.

FE simulation of crack growth rate was done by several authors [10, 11, and 12]. However the incorporation of RCF detection methods into crack propagation algorithms has not yet been explored.

This paper presents the development of an intelligent image processing algorithm capable of detecting fatigue defects from images of the rail surface. The algorithm generates statistical data (such as total number of detected defects per image, damage index of entire image, specific region of interest (ROI)). Adaptive histogram equalisation is used for the local contrast enhancement so the defect regions are clearly visible. Then an adaptive threshold method is employed to segment the defects. Geometrical properties (such as greatest length between boundary points, area, perimeter, boundary coordinates, orientation, minor and

major semi axis of each defect) are also identified. These parameters are automatically incorporated into a 3D wheel-rail crack growth model (S1002 wheel, 60E1 rail) containing the rail crack growth model. The FE model includes simulated wheel lateral displacement, roll angle, and vertical displacement extracted vehicle dynamics simulations using VAMPIRE. Estimates of Mode I and Mode II stress intensity factor (SIF) are processed in accordance with the crack growth laws to predict the crack growth rate and direction.

## 2. Image processing algorithm for detection of geometrical properties of discrete surface defects

Magel et al [13] describes the main challenges of applying image processing methods to images of rail defects, these include: inhomogeneous illumination; variation of reflection property on rail head caused by stains and rust. NRC Canada acquired rail defect images (see Figure 2) using a RAILSCOPE image acquisition system (IAS) with one camera per rail, minimum resolution of 2 Mega-pixel, field of view (FOV) 8 inch x 6 inch. The IAS is capable of acquiring blur free images at vehicle speeds up to 35 mph.

Gim Joy [14] presents the use of VIS with IAS including vibration isolators (to reduce blurring of images) and multiple cameras per rail (to increase the number of extracted geometrical features).

Figure 1 describes the steps of the image processing algorithm. The pre-processing of images is done by contrast enhancement. The local normalisation (LN) and adaptive histogram equalisation have been investigated as image enhancement techniques. Also binary segmentation by adaptive thresholding is used for crack segmentation. After the detection stage of the algorithm, the detected defects are further post-processed with image cleaning morphological operations (such as erosion and dilation of pixels, removal of false defects). Then the following geometrical properties of each defect are extracted: length (maximum distance between any two points along the boundary of the defect), orientation of the defect (orientation about x axis), area, and perimeter. The measured defect geometry is calibrated using the rail foot dimension.

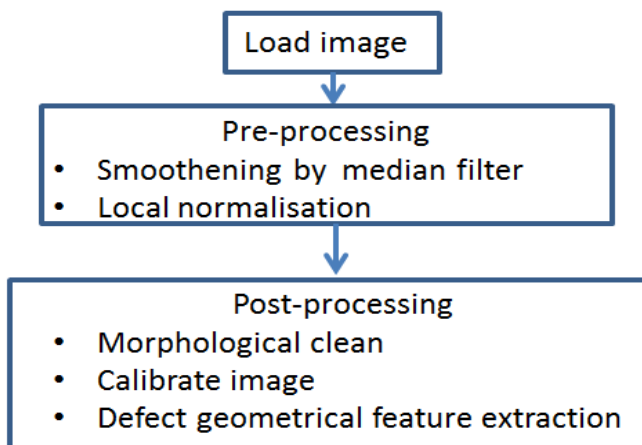


Figure 1. Image processing algorithm

Pre-processing stage – Acquired images are mostly contaminated by unwanted noise due to climatic factors and grinding marks. In rail image processing applications these non-defects abnormalities (including illumination inequality) need to be addressed prior to actual defect detection. Frequency transform methods - such as Fast Fourier Transform (FFT) - remove both noise and unwanted defects by excluding particular frequencies. However these methods are susceptible to loss of important information.

Pre-processing technique	Benefits	Limitations
Average filtering	Easy to implement and efficiently smoothens the image and removes noise.	Large size filters increase the computation time and blur image edges.
Median filtering	Masks of various shapes can be used helping to save line structures.	Cannot keep the sharpness of the image.
Gaussian smoothing	Effective reduction of noise and edge blur.	Time consuming and loss of detail in image.

Table 1. Comparison between image filtering methods

It was decided to use the median filtering technique after analysing the benefits and limitations of various techniques presented by [15] (see Table 1).



Figure 2. Filtered heavy RCF damaged rail (NRC, Canada)

The contrast enhancement of initial photo (Figure 2) is performed by using LN method which is illumination independent. Figure 3 shows the simulated results after using an efficient implementation (WxW pixel block) of the LN functionality contained within MATLAB's Image Processing Toolbox.

Locally normalized image



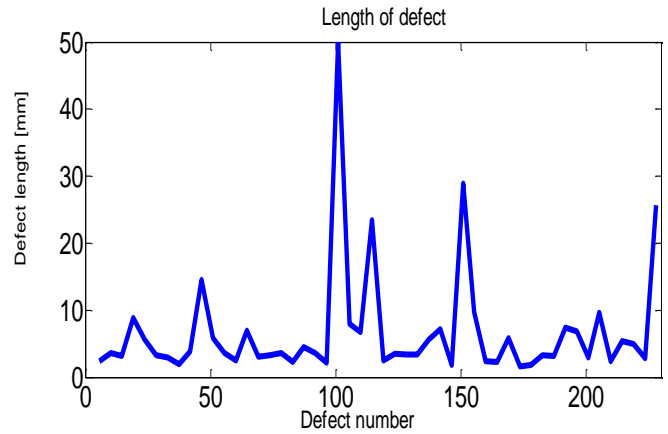
Figure 3. Result of LN applied to initial photo

**Defect processing stage** – The pre-processed image contains potential defects and other spots with local minimum gray levels. To differentiate between defects and other artefacts a number of edge detection methods were investigated, including: gradient method, Otsu method, adaptive thresholding and valley emphasis method. The Otsu method (global thresholding) though popular is biased towards the component with larger class variance or larger class probability. Adaptive thresholding [16] gives better results than the above mentioned methods but is susceptible to noise. The valley emphasis method [17] weights the objective function defined in the Otsu method with the neighbourhood gray level of the threshold, and selects a threshold value that has small probabilities in its neighbourhood area and also maximises the variance between classes in the gray-level histogram. This method is robust for images containing Gaussian noise. The segmentation threshold in this paper is estimated by automatic iterative selection.

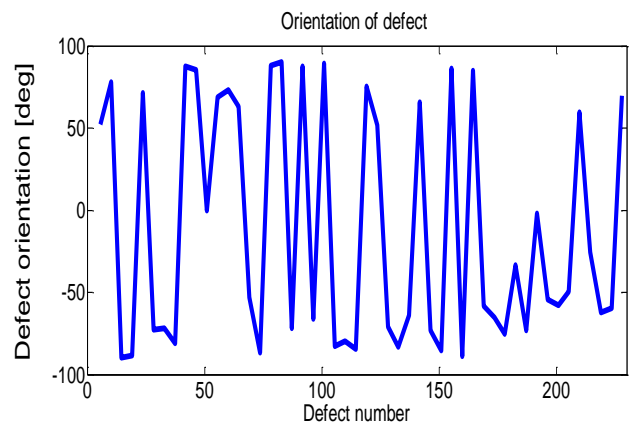
**Defect post-processing stage** – Segmented defects are further post-processed to remove most of remnant noise and/or false defects by morphology. These false defects significantly affect the efficiency of the algorithms for rail maintenance inspection. At this stage the image is combined (intersection, union, difference, reflection and complement etc.) with some structuring elements to enhance the precision of the detected defects and to reduce the background noise detected at the same time [18].

The MATLAB **'bwmorph'** command was employed to perform morphological operations on binary images. The input arguments are **'fillgap'** (to fill small gaps in edges),

**'dilate'** (to dilate the image), **'erode'** (to perform erosion), and **'remove'** (to remove interior pixels) as presented in [19]. The image processing algorithm detected 228 defects from the initial image. Figure 4 shows a maximum detected defect length of 50 mm for defect number 100 and a length of 27 mm for defect number 150.



a)



b)

Figure 4. a) Defect length b) Defect orientation

Percentile [%]	Length [mm]	Area [mm <sup>2</sup> ]	Orientation [deg]
90	7.0845	9.383	90.000
80	3.918	4.248	87.678
70	3.100	2.600	82.024
60	2.359	2.002	75.490
50	1.893	1.640	71.882
40	1.420	0.787	65.896
30	0.724	0.367	58.865
20	0.590	0.210	45.000
10	0.362	0.131	0.000

Table 2. 90<sup>th</sup> – 10<sup>th</sup> percentile of identified cracks

Further analysis of post-processed image is done for defect number 100 and defect number 150. It is obvious that the peak values for crack lengths correspond to clusters of cracks in the post-processed image. Figure 5 shows the clusters of

discrete defects detected by the developed image processing algorithm. The severity of damage for the identified clusters is calculated by using a damage index function which employs binary mask for specified regions of interest (ROI). The ratio between the area of cluster and area of binary mask estimates the level of damage (with a maximum damage index of 1).

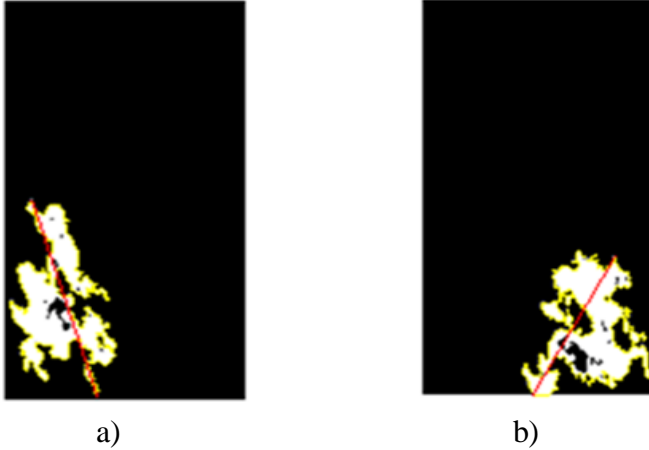


Figure 5. a) Cluster for defect 100 b) cluster for defect 150

### 3. Prediction of rail crack propagation using 3D FE model for wheel-rail interface

The quasi static simulation of wheel-rail interface is undertaken using the COMSOL software. The length of rail section is 600mm, Poisson ratio  $\nu = 0.3$  for wheel and rail materials and Young's modulus = 210 MPa. The wheel is initially positioned at the centre line of railhead and an axle load of 80 kN is applied on the wheel in load steps. An extra fine free tetrahedral mesh is used with maximum element size of 0.9 mm at the contact patch. The simulated values for wheel: vertical displacement, roll angle, and lateral displacement are included in the COMSOL model from VAMPIRE vehicle dynamics software. Afterwards these values are included in the COMSOL model. It is assumed that the lateral displacement of the right wheel is changing from central position in steps of 1mm until flange contact (see Figure 6).

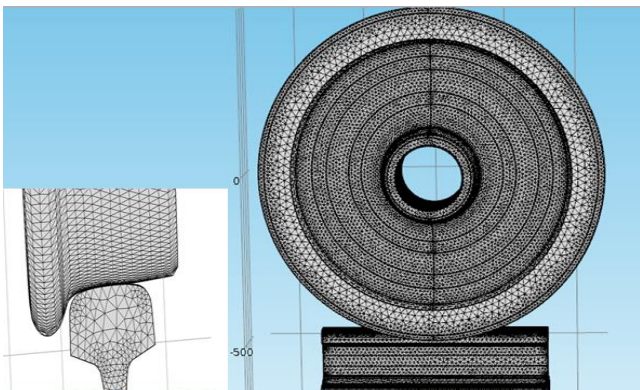


Figure 6. FE simulation of S1002 and 60E1 contact

The COMSOL simulated contact pressure is compared with the contact data generated from VAMPIRE (see Figure 7). The differences between simulated results could be due to the assumptions made by these two software packages. COMSOL software assumes that the wheel-rail interface model contains linear elastic material property, and therefore includes deformation in the contact patch. This increases the contact area and reduces the stresses. The VAMPIRE software assumes the wheel and rail material as being rigid and no deformation is included in the contact patch. As a result, the VAMPIRE contact data tends to be higher than the COMSOL data. The normal force at the contact patch appreciates as lateral displacement increases (as the wheel moves towards flange contact), due to the influence of contact angle. This corresponds to an increase in contact pressure and decrease in contact area in both models. The simulated results show the influence of non-linear effects as the wheel approaches flange contact for lateral displacements greater than 5mm.

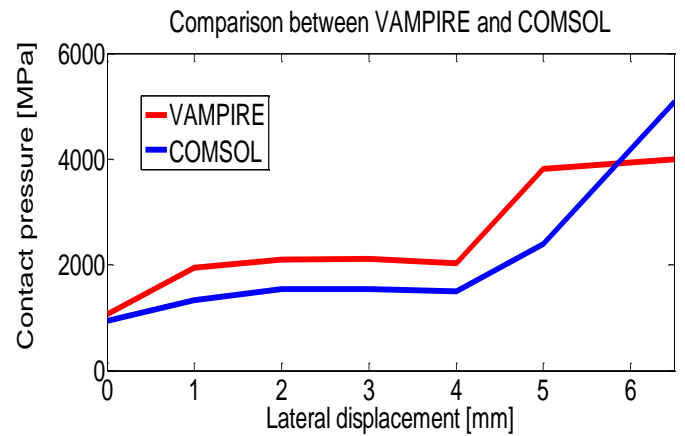


Figure 7. Validation of 3D FE contact model

Evans et al [20] presented a flexible track model including the flexibility of rail track, sleeper mass, resilience of railpad, fastening elements and ballast stiffness. The rail length in between sleepers and sleeper spacing should be considered in the sensitivity analysis of the flexible track model.

This paper describes an FE model for wheel-rail interface including sleeper mass and the stiffness and damping of rail pad and ballast (see Table 3).

Parameter	Value
Rail pad stiffness	200E6 [N/m]
Rail pad damping	50E3 [N.s/m]
Sleeper mass	314 [Kg]
Ballast stiffness	125E6 [N/m],
Ballast damping	310E3 [N.s/m]

Table 3. Details of rail supporting structure. [21]

The influence of including the rail substructures is observed to lower the contact pressure by only few MPa (approximately 3.173 MPa) when the rail substructures are included in the model. Also the total displacement of the rail is observed to increase to approximately 0.098 mm in the vertical direction. This can be attributed to the spring stiffness



and damping constant of the combined structures, which offer the rail more bending moment (see Figure 8). The increase of space between sleepers generates higher reaction forces and displacements in rail [20]. While increase in railpad stiffness decreases displacement of rail with a slight increase in support interaction forces. The contact forces at the wheel-rail interface are observed to decrease for decreasing ballast damping constant, as reported by Zakeri et al [22].

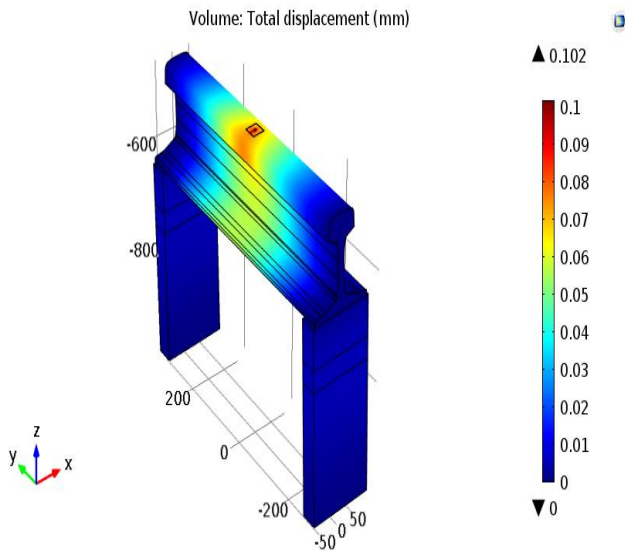


Figure 8. COMSOL simulated results for rail supported by pads, sleepers and ballast

Finally a sensitivity analysis of the FE contact model at central position (0 mm lateral displacement) in relation to applied load is carried out. The contact pressure is directly proportional to the applied load due to linear elastic nature of the wheel and rail materials.

### 3.1 Stress intensity factor estimation and crack growth rate calculations

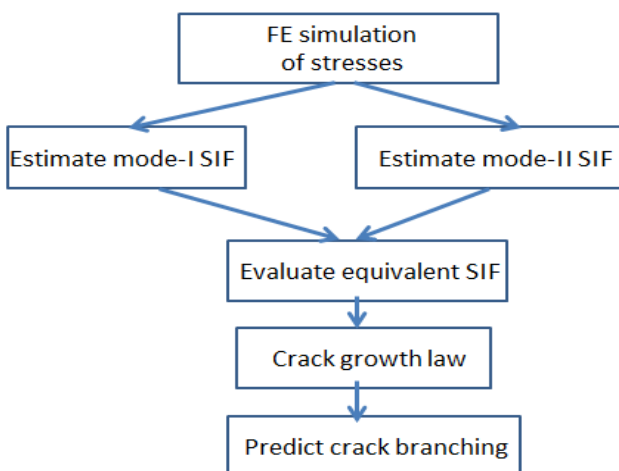


Figure 9. Fracture mechanics model

The detailed crack propagation model utilises the Stress Intensity Factor (SIF) estimation based on the J-integral method. The relevant stress components are decomposed within a closed loop contour around the crack tip into modes I, II and III. The paper focuses on modes I and II (dominant loading modes on rail RCF).

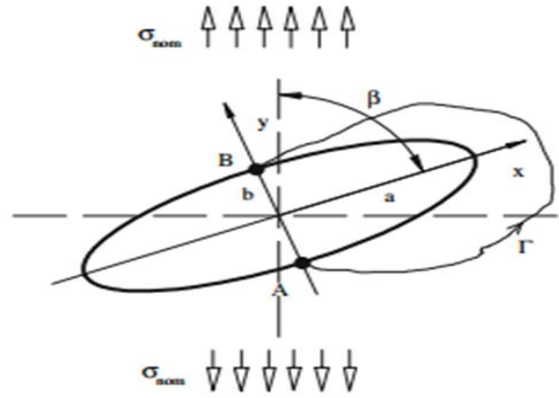


Figure 10. Inclined elliptical crack [20]

Paolo, S Fausto [23] use J-integral method to calculate mode I SIF at the tip of the crack for a generic inclination angle  $\beta$  as follows:

$$J_I = \frac{K_I}{E'} = \frac{\sigma_{nom} \pi a}{E'} \sin^2(\beta) \quad (1)$$

where:  $\sigma_{nom}$  is nominal stress component,  $K_I$ : mode-I SIF,  $E'$  is the shear modulus,  $J_I$ : J-integral for mode-I,  $a$  is crack major semi axis,  $b$  is minor semi axis of crack,  $c = \sqrt{a^2 - b^2}$ . The estimated mode I SIF for different crack inclination angles and axle loads is presented in Figure 11. As expected the largest Mode I SIF is calculated with a 90° crack angle.

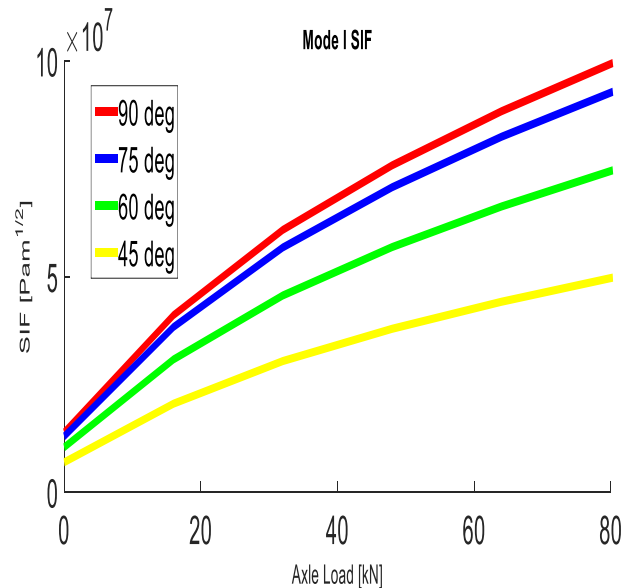


Figure 11. Estimated SIF for Mode I fracture

Mode-II SIF at the tip of the crack is estimated using the following equations:

$$J_{II} = \frac{K_{II}}{E'} = \frac{\sigma_{nom}\sqrt{\pi a}}{E'} \sin(\beta)\cos(\beta) \quad (2)$$

where:  $\sigma_{nom}$  is nominal stress component,  $K_{II}$ : mode-II SIF,  $E'$  is the shear modulus,  $a$  is crack major semi axis,  $b$  is minor semi axis of crack,  $c = \sqrt{a^2 - b^2}$ . The estimated mode II SIF for different crack inclination angles and axle loads is presented in Figure 12. Note that zero Mode II SIF is calculated for 90° crack angle due to the orientation of the crack relative to the applied load.

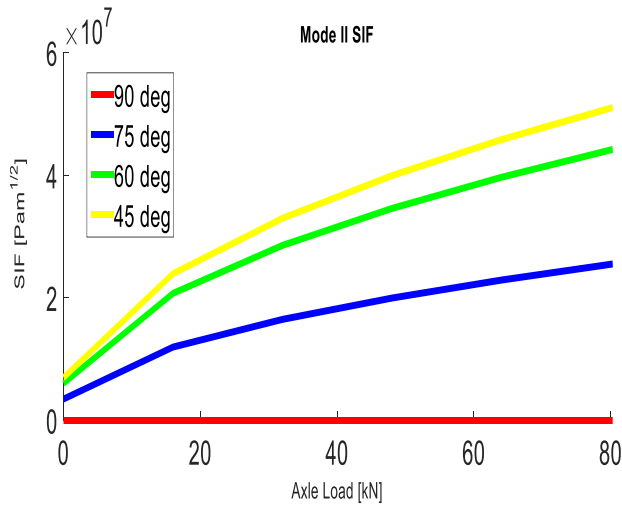


Figure 12. Estimated SIF for Mode II fracture mode

Lewis and Olofsson [24] presented crack growth laws for RCF cracks on rails after extensive testing using biaxial fatigue specimens of normal grade rail steel cut from the rail web. Equation (5) calculates the change in equivalent SIF which is used to formulate the mixed mode loading of modes I and II SIF. The equivalent SIF will be used to estimate growth rate due to combined fracture modes I and II.

$$\Delta K_{eq} = \sqrt{\Delta K_I^2 + \left[\frac{614}{507} \Delta K_{II}^{3.21}\right]^2 / 3.74} \quad (3)$$

Where

$\Delta K_{eq}$ : is change in equivalent SIF

$\Delta K_I$ : change in mode I SIF

$\Delta K_{II}$ : change in mode II SIF

### 3.2 Incorporating defect detection algorithm with FE wheel – rail model

This section presents the automatic incorporation of defect detection algorithm results into the wheel-rail contact model. The growth rate of the defect is estimated based on linear elastic fracture mechanics (LEFM). The link between defect detection algorithm and wheel-rail contact model could contribute to the enhancement of the maintenance procedures for rails. Two separate tasks - detection and prediction of critical rail damage – can be combined.

The LiveLink™ for MATLAB enables the exportation of COMSOL global expressions to MATLAB workspace and vice versa. This allows the simulated values from COMSOL wheel-rail contact model (including the rail crack) to be imported in MATLAB. The steps for linking the MATLAB defect detection algorithm to 3D COMSOL crack growth model are as follows:-

Step 1 – Run image processing algorithm

Step 2 – Select a defect of interest

Step 3 – Use LiveLink™ to integrate COMSOL (FE) with MATLAB (image processing)

Step 4 – Run integrated COMSOL model

Step 5 – Predict crack growth rate and orientation in MATLAB and COMSOL.

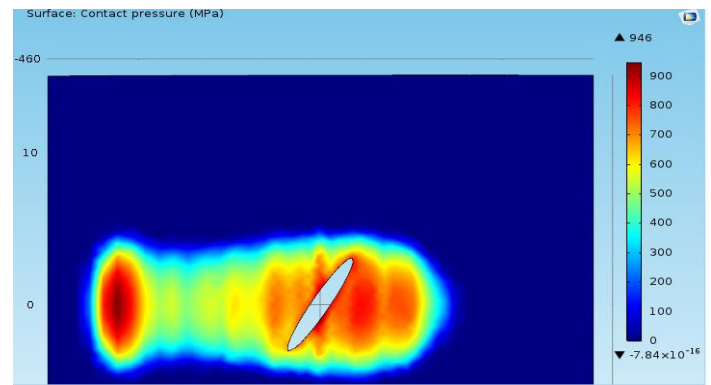


Figure 13. COMSOL results after linking the defect detection algorithm with 3D crack growth model

Figure 13 shows how the elliptical equivalent crack (detected by the image processing algorithm) is automatically incorporated within the 3D FE wheel-rail contact model. The major, minor axis and orientation are exported to COMSOL from MATLAB using the LiveLink™.

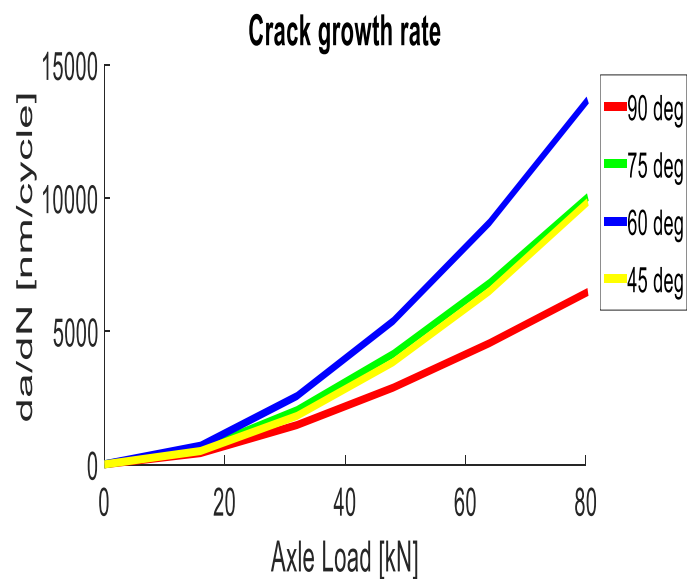


Figure 14. Surface crack growth rate

The crack growth rate is estimated as a function of stresses where cracking is inclined at an angle to the applied load [21], as detailed in Equation (6). This paper considers a case study of crack orientation ranging from:  $\frac{\pi}{4} < \beta < \frac{\pi}{2}$ .

$$\frac{da}{dN} = 0.000507(\Delta K_{eq}^{3.74} - \Delta K_{th}^{3.74}) \quad (4)$$

Where

$\frac{da}{dN}$ : crack growth rate  
 $\Delta K_{th}$ : change in SIF threshold

The growth rate of inclined cracks as shown in Figure 14 indicates an increase in surface growth rate as inclination angle decreases for an elliptical crack with major axis length of 3.5 mm and minor axis length of 0.5 mm. Similar conclusion has been presented in [27].

The overall crack growth direction for the inclined elliptical crack is determined by the dominant tensile (or shear equivalent SIF) as shown in [21].

$$\theta = 2 \times \text{atan}\left(\frac{K_I - \sqrt{K_I^2 + 8K_{II}^2}}{4K_{II}}\right) \quad (5)$$

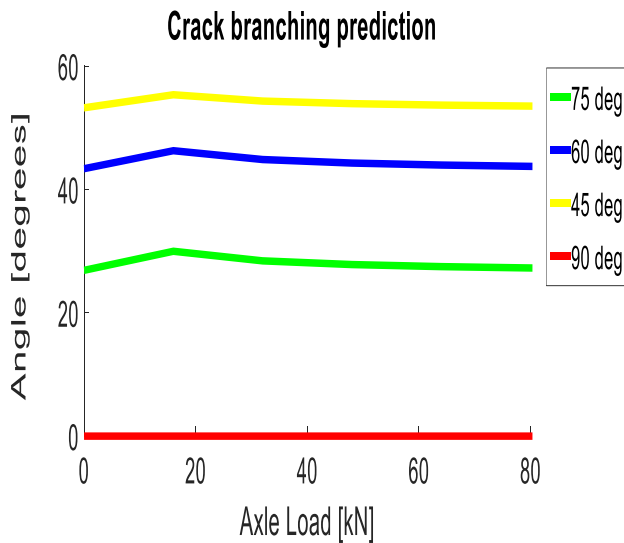


Figure 15. Surface crack growth direction

The surface direction of propagation (see Figure 15) confirms that for tensile loading case, the highest branch angle is observed at mixed I and II fracture modes (when  $K_{II}$  is maximum i.e.  $\beta = \frac{\pi}{4}$ ). While the symmetry of the deformation in mode I loading (where  $\beta = \frac{\pi}{2}$ ) implies that the crack growth direction can only be perpendicular to the direction of applied load [26].

Further development of the integrated defect detection algorithm and crack growth model will focus on the monitoring/prediction of the actual surface condition of rail head. This will include the incorporation of more realistic vehicle, loading, and environmental characteristics. Also, the application of the developed algorithms for real-time condition monitoring will be investigated by simplifying the

assumption of the FE contact model (linear elastic model accounting for deformation in the contact model), which is already known to be time consuming as compared to Hertz theory (rigid bodies in contact with no deformation).

## 4. Conclusions

Visual inspection systems (VIS), though susceptible to the reflection property of rail head (specular or diffuse), have advantages (e.g. fast computational time) over other monitoring techniques for the detection of rail surface condition. The paper described the development of a VIS which combines an intelligent image processing algorithm, capable of detecting fatigue defects from images of the rail surface, with a FE crack growth model. The computational requirements of the combined model (surface defect detection and fracture mechanics) can be summarised as shown in Table 4 below. Although the high computation requirement of the fracture mechanics model can be reduced considerably with larger mesh size's (at the expense of accuracy). Further investigation of alternative means of estimating the contact stresses and strains will improve the readiness level of this application being adopted in industry.

Component	Computational time	Speed
RAILSCOPE IAS	40-60 $\mu$ second (static-dynamic shutter speed)	High
Image processing algorithm	1.055 seconds (including idle time)	Medium
Fracture mechanics model	4hr 35mins 21 secs (At 0.9mm rail head element size)	Slow

Table 4. Computational requirements of integrated model

During the development of the image processing algorithms, the adaptive histogram approach to image enhancement was shown to give the best results as compared with other enhancement techniques such as, FFT and normalisation methods. Also, the adaptive thresholding method used in this research work shows good correlation with Otsu's segmentation. Regions of the defect image (original) that are corrupted by excess illumination on the rail head makes individual defect detection in those regions impossible, rather in such regions, clusters of defects are observed.

Validation of FE wheel-rail contact model shows good agreement with the VAMPIRE contact data (approximately 12% variation at mesh size of 0.9mm). The variation in the results is proportional to the mesh size, simulation time and assumptions in the wheel-rail contact algorithms. Comparing the SIF obtained from the analytical solution of the J-integral



method in COMSOL and that presented by Dhalberg and Ekberg [25] shows good agreement. The estimated SIF (mode I and mode II) are combined to estimate the surface crack growth rate and surface direction.

The results of this study verify the potential benefits of linking non-destructive rail inspection techniques to detailed crack growth prediction model. This paper serves as an initial study demonstrating the viability of the proposed incorporation of non-destructive inspection methods to crack growth models aimed at improving safety of operations and maintenance requirement in terms of damage levels and critical defect length predictions. The current work is to be further developed to explore more links that can be established between other non-destructive inspection methods of rail condition and crack growth models. Automated validation of measured geometrical features of each detected defect will also be required. This may include comparison of the simulated results to actual field measurements of crack growth over a known time interval.

Investigation and inclusion of fluid structure interaction is essential to the overall aims of research. This will enable the critical understanding of crack propagation under different environmental conditions. Ways to improve the developed algorithm, enabling detection of individual cracks within a cluster of defects. Further comparison of the COMSOL model with other available contact models, such as FastSim and CONTACT, will also be carried out. Finally, optimisation of the incorporated model (image processing, wheel-rail contact and fracture mechanics) is essential. This will include a sensitivity analysis of each component of the integrated model to its influential parameters and will elaborate on the practical limitations of this approach to non-destructive rail inspection in industry.

## Acknowledgment

The Authors will like to acknowledge the support of National Research Council (NRC) Canada and Institute of Railway Research from the University of Huddersfield, U.K.

## References

- [1] Network Rail. (2016). Network Rail Technical Strategy. Retrieved from <https://www.networkrail.co.uk/publications/technical-strategy>
- [2] Papaalias, M. P., Roberts, C., Davis, C. "A review on non-destructive evaluation of rails: state-of-the-art and future development". In *Part F: Journal of Rail and Rapid Transit IMechE Proceedings*, vol. 222, no 4, pp. 367-384, 2008.
- [3] Innotrack, (2008). D4.4.1 Rail Inspection Technologies. Retrieved from <http://www.innotrack.net/IMG/pdf/d414.pdf>
- [4] Hashmi, MF. Avinash, G K. "Computer-Vision Based Visual Inspection and Crack Detection of Railroad Tracks" In *IEEE 5<sup>th</sup> Int. Conf on Soft computing and pattern recognition*, vol 1, no. 1 pp-228-236, 2013.
- [5] Zhang, W. Zhang, Z. Qi, D. Yun, Liu. "Automatic Crack Detection and Classification Method for Subway Tunnel Safety Monitoring". In *Sensors*, vol 14, no 10, pp. 19307–19328, 2014.
- [6] Quingyong Li, & Shengwei Ren. "A visual detection system for rail surface defects". In *Systems, Man, and Cybernetics, Part C: Applications and Reviews, IEEE Transactions*, vol 42, no 6, pp. 1531-1542, 2012.
- [7] Jyoth, RL. Gimy, J. "A Real Time VIS for Rail Flaw Detection. In *Intl Journal of Scientific Research and Publication*, vol 4, no 8, 2014.
- [8] Ze Liu, Wei Wang, Xiaofei Zhang, Wei Jia. "Inspection of Rail Surface Defects Based on Image Processing". In *IEEE 2nd Int Asia Conf Informatics in Control, Automation and Robotics*, vol 1, no 1, pp. 472-475, 2010.
- [9] Zhendong, H. Yaonan, W. Feng, Y. Fie Liu. "Surface defect detection for high speed rails using inverse P\_M diffusion model". In *Sensor*, vol 31, no 1, pp. 86-97, 2016.
- [10] Popovici, R. "Friction in Wheel-Rail Contacts" PhD thesis, University of Twente, Enschede, 2010.
- [11] Brouzoulis, J. Ekh, M. "Crack propagation in rails under rolling contact fatigue loading" *International Journal of Fatigue*, 2012, 45,(1), pp.98-105.
- [12] Trolléa, B. Baiettoa, A. Gravouila, S.H. Maib, T.M.L. Nguyen-Tajarb. "XFEM crack propagation under rolling contact fatigue". In *Procedia Engineering*, vol 66, no. 1, pp. 775 – 782, 2013.
- [13] Magel, E. "Quantifying Surface Damage Task" In *International Collaborative Research Initiative (ICRI)*, 2015.
- [14] Gimmy, J. Hyfa, N. Remya, K. "Rail flaw detection using image processing concepts-A review". In *Int J Eng Research and Technology*, vol 3, no 4, 2014.
- [15] Javed, A. Ashfaq Qazi, K. Maqsood, M. Ali Shah, K. "Efficient Algorithm for Railway Tracks Detection Using Satellite Imagery". In *Int. J Image, Graphics and Signal Processing*, vol 11, pp. 34-40, 2012.
- [16] Malik, Qurrat-ul-Ain. "Novel methods of object recognition and fault detection applied to non-destructive testing of rail's surface during production". PhD thesis, Manchester Metropolitan University, 2013.
- [17] Jiu-Lun, F. Bo, L. "A modified valley-emphasis method for automatic thresholding". In *Pattern Recognition Letters*, vol 33, no 6, pp. 703–708, 2012.
- [18] Wilson T. Wamani & Villar, C. "Aurora Automated Railroad Tie Condition Assessment System: The Quest for Accuracy". In *AREMA Annual Conference & Exposition*, George Town Rail Equipment Texas, 2009.
- [19] Ledda, A. "Mathematical Morphology in Image Processing", PhD thesis Ghent University, 2007.
- [20] Evans, G., Shahzad, F., de Vries, E., Cavalletti, M., Iwnicki, S. and Bezin, Yann "An investigation of sleeper voids using a flexible track model integrated with railway multi-body dynamics" In *Proc. of IMechE, Part F: Journal of Rail and Rapid Transit*, vol 223, no. 6. pp. 597-607, 2009.
- [21] Vo, K D. Tieu, A.K. Zhu, H.T. Kosasih, P.B. "A 3D dynamic model to investigate wheel–rail contact under

- high and low adhesion” In International Journal of Mechanical Sciences, Elsevier, vol 85, pp. 63–75.
- [22] Zakeri, A.J. Xia, H. “Sensitivity of track parameters on train track dynamic interaction” In Journal of Mechanical Science and Technology, vol 22, pp. 1299-1304, 2008.
- [23] L Paolo, L. Fausto, S. ”Analytical evaluation of J-integral for elliptical and parabolic notches under mode I and II loading” Int Journal of Fracture, vol 148, pp.57-71, 2007.
- [24] Lewis, R. Olofsson, U.: ‘Rail Surface Fatigue and wear’ in ‘Wheel-rail interface handbook’: (Elsevier Press 2009, 2<sup>nd</sup> edn.), pp. 280-308.
- [25] Dhalberg, T. Ekberg, A.: ‘Stresses, stress concentration, stress at crack tip, stress intensity factor, fracture criteria’, in ‘Failure Fracture Fatigue’ (Sweeden, Studentlitteratur Press, 2002, 1st edn.), pp. 71–77.
- [26] Patricio, M. Mattheij, R.M.M. “Crack propagation analyses” Published in Technische University, Eindhoven, 2007, pp. 22.
- [27] Naresh, M.K. Chetan, S.J. “Investigation of fatigue crack growth under pure mode I and mixed mode” In Int’l Journal of Engineering Research and Technology, vol , no. 5, pp. 765-771, 2015.

University of Huddersfield, UK. She has been conducting research on several EU projects – Automain, Sustrail and Capacity4rail. She is the author of over 100 refereed publications and reviewer for several internationally leading journals. Crinela is Chair of IET West Yorkshire network, member of the executive board for IET Yorkshire region and representative for Women in Engineering Society (WES). She has an active current profile in internationally leading research on control engineering, intelligent sustainable autonomous rail vehicles, real time traction control, rail vehicle-track interaction, integrated system analysis for controlled vehicles, multibody non-linear system dynamics, mechatronics and Engineering education.

## Authors



**Bello Sambo** graduated in 2014 attaining an MSc with distinction for his thesis “Modelling and Simulation of the Twin Disk Rig with Experimental Validation” at the University of Huddersfield, UK. Previously he had graduated with Honours degree in Electrical and Electronics Engineering with specialisation in Communications Engineering at Eastern Mediterranean University TR Northern Cyprus. He joined the Institute of Railway Research full time in April 2014 to begin a PhD programme. His research interests include intelligent rail RCF condition monitoring systems aiming to improve maintenance team planning.



**Dr Adam Bevan** - Following the completion of his PhD in 2004, Adam joined the Rail Technology Unit at Manchester Metropolitan University. During his time at the Rail Technology Unit, Adam built up a wide range of expertise and knowledge in the field of wheel-rail interface engineering, vehicle dynamics simulation and vehicle-track interaction. Adam joined the University of Huddersfield in July 2012 where he is currently Head of Enterprise for the Institute of Railway Research. Currently Adam is leading a number of industry sponsored research and enterprise projects for various industrial clients. Current research includes the investigation of the causes, prediction and mitigation of wear and RCF on both wheels and rails.



**Dr. Crinela Pislaru** is Senior Lecturer in the Engineering and Technology department at the